UDC 539.4

Cyclic Plastic Response and Damage in Materials for High Temperature Applications*

J. Polák,[a,b] K. Obrtlík,[b] and M. Petrenec[b]

[a] Institute of Physics of Materials, Academy of Sciences of the Czech Republic, Brno, Czech Republic

[b] CEITEC IPM, Institute of Physics of Materials, Academy of Sciences of the Czech Republic, Brno, Czech Republic

УДК 539.4

Циклическое пластическое деформирование и повреждение материалов при высоких температурах

Я. Полак[а], К. Обртлик[б], М. Петренец[б]

[а] Институт физики материалов АН Чехии, Брно, Чехия

[б] CEITEC научный центр Института физики материалов АН Чехии, Брно, Чехия

Анализ кривых гистерезиса показывает, что при различной температуре имеют место характерные изменения зависимости между циклическими пластическими деформациями и напряжениями в нержавеющей стали и суперсплавах. Соответствующее изменение микрорельефа поверхности при мягком нагружении зафиксировано с помощью сканирующей и томографической электронной микроскопии с высоким разрешением. Проанализированы механизмы локализации циклической деформации, образования поверхностного микрорельефа, инициирования усталостных трещин и роста коротких трещин.

Ключевые слова: усталостное повреждение, циклическая пластичность, инициация трещины, высокая температура, нержавеющая сталь, никелевый суперсплав.

Introduction. Stainless steels and nickel-based superalloys are often used for design of numerous high-temperature components, e.g., energy production or aircraft turbines. The critical parts of the components are subjected to repeated elastic-plastic straining as a result of heating and cooling during start-up and shutdown periods [1, 2]. Thermal stresses produce appreciable variable thermal strains and result in appearance and growth of fatigue cracks. Low-cycle fatigue properties of these materials thus represent an important consideration in the design of the components.

The study of the low cycle fatigue behavior of these materials was concentrated mostly to the analysis of the stress–strain response, internal structures, fatigue life and crack growth [1–3]. In recent years, considerable attention has been attracted to the study of the early damage mechanisms in crystalline materials, starting with the cyclic slip localization and resulting finally in the initiation of fatigue cracks and their early growth [4, 5].

In this contribution, the methods allowing to study the sources of cyclic stress and early fatigue damage at room and elevated temperatures are presented and used to reveal details of the mechanisms of cyclic plastic straining and fatigue damage evolution in austenitic steels and nickel superalloys.

---

* Report on International Scientific Conference “Fatigue and Thermofatigue of Materials and Structural Components” (Kiev, 2013).

1. **Cyclic Plastic Stress–Strain Response**. Cyclic plasticity of materials is usually studied in strain-controlled cycling with constant strain rate, since stress response of the material depends not only on temperature but also on the strain rate. In a standard low cycle fatigue experiment, several specimens are cycled in a symmetrical cycle with constant total or plastic strain amplitudes, and their stress response is recorded and evaluated. Hysteresis loops can be stored in computer memory, and stress, strain and plastic strain amplitudes are evaluated during the fatigue life. The plot of the stress amplitudes vs. number of loading cycles represents the fatigue hardening/softening curves. The plot of the saturated stress amplitude (or stress amplitude at half-life) vs. strain or plastic strain amplitude represents the cyclic stress–strain curve.

In order to find the sources of the cyclic stress, more detailed analysis is necessary. Hysteresis loop and the analysis of its shape using the generalized statistical theory [6] can yield information on the sources of the cyclic stress and its variation with temperature. The formulation of the statistical theory of the hysteresis loop uses the original Masing approach [7] extended later by Afanas'ev [8], according to which the crystal can be represented by a parallel arrangement of microvolumes having different internal critical stresses. The generalized statistical theory [6] considers not only the internal stress but also thermally activated component – effective stress. The analysis of the loop shape allows separating the contributions of the effective stress and internal stress. The probability density function of the internal critical stresses can be evaluated. This approach has been applied to carbon steel cycled at room and depressed temperatures [9], to austenitic, ferritic and duplex stainless steels [10, 11], and also to nickel superalloys [12]. The probability density function can be compared with the internal dislocation structure developed in cyclic straining and allows thus obtaining the deeper insight into the mechanisms of cyclic plastic straining.

Figure 1 shows the hysteresis loop of austenitic 316L steel cycled at room temperature and the first and second derivatives of the compression half-loop plotted vs. $\varepsilon_r E_{eff}/2$, i.e., vs. fictitious stress. Since austenitic steel is a single-phase material, the interpretation of the plot of the first and second derivatives vs. fictive stress is simple. The initial drop of the first derivative and also of the second derivative to its minimum corresponds to the decrease of the effective stress after reversal of the strain. The x coordinate corresponding to the minimum of the second derivative corresponds to the saturated effective stress $\sigma_{es} \sim$ 40 MPa. Beyond this value the second derivative approximates the probability density function of the internal critical stresses $f(\sigma_{ic})$ according to the relation [6]

$$f(\varepsilon_r E_{eff}/2 - \sigma_{es}) = -\frac{2}{E_{eff}^2}\frac{\partial^2 \sigma_r}{\partial \varepsilon_r^2}, \tag{1}$$

where σ_{es} is the saturated effective stress and E_{eff} is the effective elasticity modulus equal to the first derivative of the loop at fictitious stress, for which the second derivative reaches its minimum. In ramp loading, the strain rate during the half-cycle is constant and saturated effective stress is constant too. The probability density function is thus obtained from the second derivative of the half-loop only by shifting the origin of the coordinate [see relation (1)].

Nickel-based superalloys are able to keep their strength up to high temperatures. The excellent high-temperature mechanical properties of these alloys arise mostly from the presence of two phases – a face-centered cubic γ matrix and γ' Ni_3Al-based precipitates with ordered $L1_2$ structure. The two-phase structure has an important effect on the hysteresis loop and its shape. In constant strain amplitude loading of IN738LC superalloy, stress amplitude was saturated. Figure 2a shows the saturated hysteresis loops of IN738LC superalloy at room and elevated temperatures. The decrease of the stress amplitude in cycling at temperature 800°C is only small.

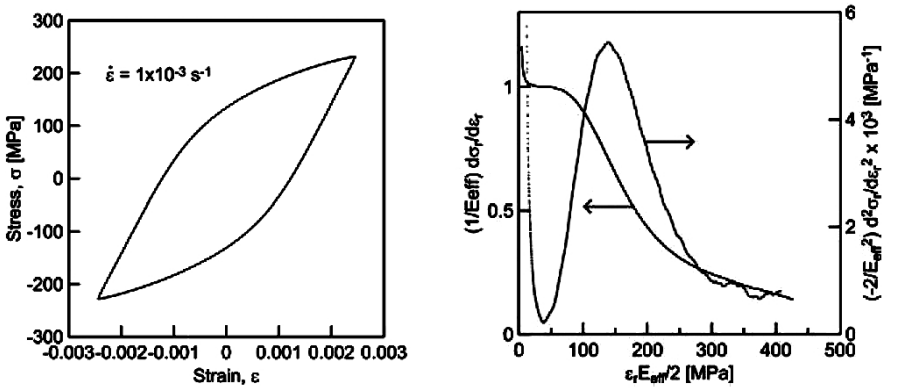

a b

Fig. 1. Hysteresis loop of 316L steel and its derivatives in constant amplitude strain-controlled cycling (a) hysteresis loops with ramp waveform (b) the first and the second derivatives of the compression hysteresis half-loop.

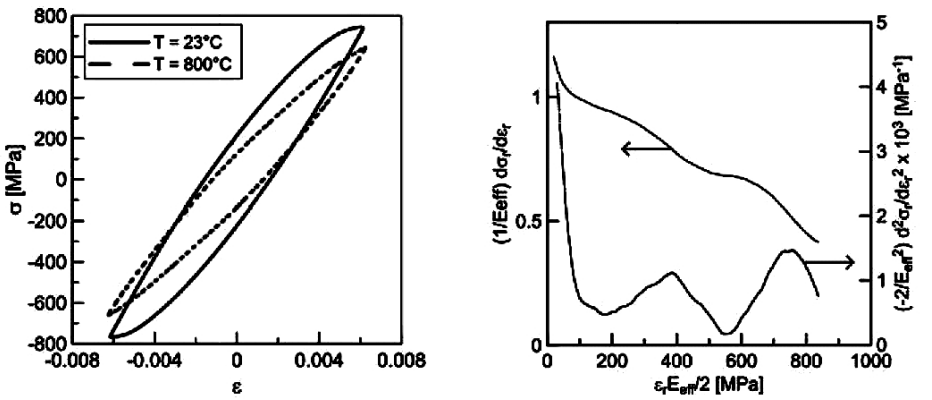

a b

Fig. 2. Hysteresis loops of IN738LC and its derivatives in constant amplitude strain-controlled cycling (a) hysteresis loops at two temperatures (b) the first and the second derivatives of the compression hysteresis half-loop at 800℃.

Both hysteresis loops were analyzed. Figure 2b shows the first and the second derivatives of the compression half-loop at 800℃. The second derivative has two separate peaks corresponding to subsequent deformation of two phases during half-cycle. The first peak, centered at fictitious stress 400 MPa, corresponds to the deformation of the matrix. The second peak, centered at fictitious stress 750 MPa corresponds to the deformation of the γ' precipitates. From the positions of both peaks we can estimate the effective stresses in both phases. From the shift of the respective distribution functions (approximated by Weibull distribution) from the origin [see Eq. (1)] the effective stresses of both phases at temperature 800℃ were evaluated $\sigma_{eff,\gamma,800} = 150$ MPa, $\sigma_{eff,\gamma',800} = 550$ MPa. Similar analysis of the hysteresis loops produced at room temperature (RT) cyclic straining led to the values $\sigma_{eff,\gamma,RT} = 90$ MPa, $\sigma_{eff,\gamma',RT} = 660$ MPa.

2. **Early Fatigue Damage**. Cyclic plastic straining of superalloys results in the formation of a pronounced surface relief similar to that found in other crystalline materials [5, 13, 14]. The surface relief has been studied most intensively at room temperature, since

surface observations are not hindered by oxidation products as in high-temperature cyclic loading. The characteristic features of the surface relief are persistent slip markings (PSMs) produced by cyclic elastoplastic loading at room and elevated temperatures [14, 15]. PSMs at the surface of a grain of IN738LC superalloy cycled with a constant strain amplitude is shown in Fig. 3. PSMs run parallel to the traces of primary {111} crystallographic plane. Detail of PSMs in Fig. 3b reveals that they consist mainly from thin extrusions of a variable height. They intersect both the austenitic matrix and γ' precipitates. Further cyclic straining leads to the growth of extrusions, production of intrusions, and finally to fatigue cracks.

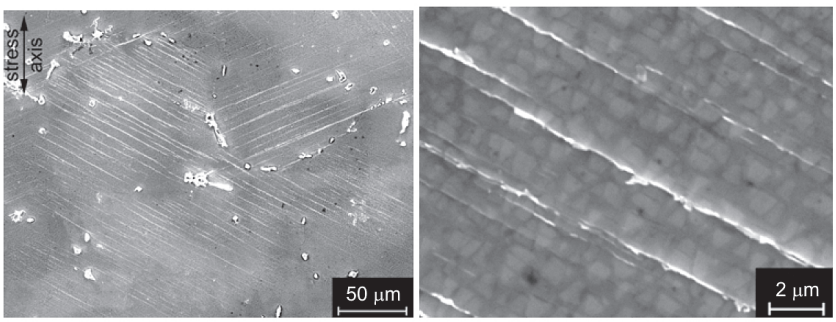

a b

Fig. 3. Persistent slip markings on the surface of the IN738LC superalloy cycled at 24℃ with strain amplitude $4.9 \cdot 10^{-3}$, $\varepsilon_{ap} = 1.4 \cdot 10^{-3}$: (a) PSMs in surface grains; (b) detail of the PSMs in Fig. 3a.

PSMs in nickel superalloys cycled at high temperatures exhibit an appreciable variability. Fig. 4 shows the surface relief of a grain of IN738LC alloy cycled at 800℃. Several parallel PSMs are present in the grain. The detailed image in Fig. 4b reveals that, in spite of the coverage of the surface by small oxide particles, characteristic features of PSM can be distinguished. Central extrusion in Fig. 4b is accompanied by two thin parallel intrusions at the interface with the matrix. This geometry is equivalent to those observed in room temperature cyclic straining of numerous crystalline materials [5]. It is expected that only one of these two intrusions will be transformed into a shallow crack and will grow through the depth of the material. The presence of intrusions and initiated cracks close to the extrusion cutting the oxidized precipitates suggest that mechanisms based on cyclic slip localization operates also at high temperatures [5].

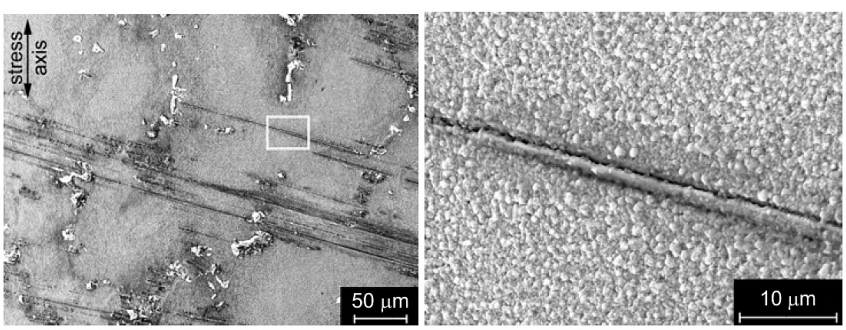

a b

Fig. 4. Persistent slip markings on the surface of the IN738LC superalloy cycled at 800℃ with strain amplitude $6.3 \cdot 10^{-3}$, $N_f = 195$ cycles: (a) overall view, (b) detail of the PSM denoted by rectangle in Fig. 3a.

The surface reliefs in superalloys cycled at room and elevated temperatures are closely related to the dislocation structure developed in the surface grains. Figure 5 shows TEM micrographs of the dislocation structure of IN713LC superalloy cycled at room temperature and at 800°C. In both cases, persistent slip bands (PSBs) with high dislocation density run parallel to {111} slip planes and intersect both the matrix and γ' precipitates. These bands usually have a specific dislocation structure, being different from that of the matrix [3, 5]. When the PSBs emerge at the surface, the PSMs arise in the form of extrusions and intrusions. The highest dislocation density is present at both boundaries of the band with the matrix (Fig. 5). The dislocation structure inside the band often reminds the ladder-like dislocation structure of PSBs in cycled copper [5]. The origin of PSMs is thus the localization of the cyclic plastic strain into PSBs. Cyclic plastic strain is localized into thin bands running parallel to the low index crystallographic planes that correspond to primary slip planes in individual grains.

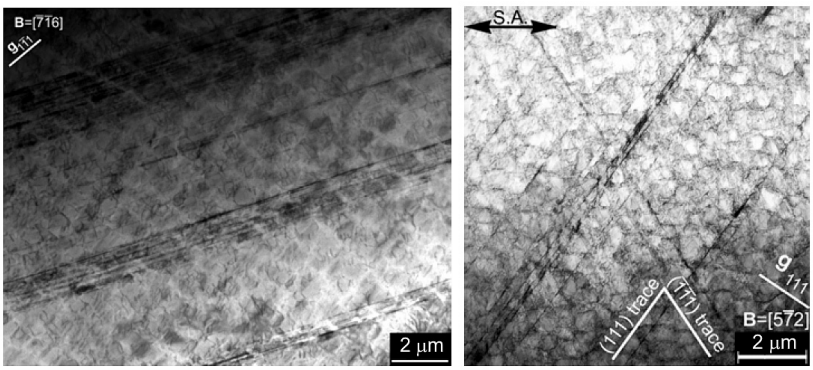

a b

Fig. 5. Dislocation structure in IN713LC superalloy: (a) cycling at room temperature, $\varepsilon_a = 5 \cdot 10^{-3}$; (b) cycling at 800°C, $\varepsilon_a = 8 \cdot 10^{-3}$.

In spite of numerous microscopic fatigue cracks initiated in PSMs, the majority of macroscopic fatigue cracks initiated in high temperature cyclic straining of nickel-based superalloys have arisen at the grain boundaries and in interdendritic areas. Figure 6 shows the early crack growth following the grain boundary path. At the tip of the growing short crack several PSMs are observed. They have the origin in PSBs steadily produced in the plastic zone of the growing crack and contribute to the early growth rate of the macroscopic crack under general yield conditions.

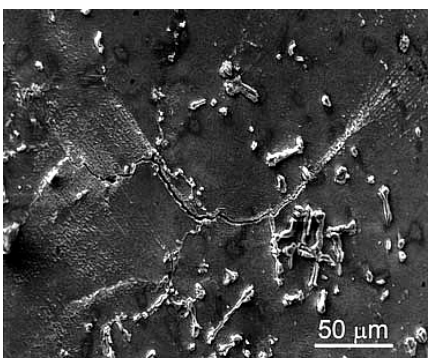

Fig. 6. SEM image of initiated crack in IN738LC superalloy cycled at temperature 700°C, $\varepsilon_a = 4.5 \cdot 10^{-3}$, $N_f = 330$ cycles.

Experimental observations performed on the cycled nickel superalloys show that localized cyclic straining results in the formation of PSBs and PSMs, both for room and high-temperature cyclic straining. Fatigue cracks can initiate in PSMs and grow. Nevertheless, the more important locations for fatigue crack initiation in high temperature cyclic straining become the grain boundaries and interdendritic areas, which often contain some eutectics and other defective structures. Fatigue crack follows an intricate crack path along these locations, contrary to the prediction of fracture mechanics. Also stress concentration at the pores and defects enhances fatigue crack initiation.

3. **Discussion**. High cyclic stress of the nickel-based superalloys is due to the presence of γ' precipitates of the type Ni_3Al with ordered $L1_2$ structure embedded in the face-centered matrix. Superdislocations in γ' precipitates can transform into an ordered structure only under effect of a very high effective stress. They are usually split with the band of antiphase and also two bands of stacking faults. The analysis of the hysteresis loop revealed low effective stresses of the γ matrix (90–150 MPa) and high effective stresses in γ' precipitates (550–660 MPa). The effective stress in γ' precipitates slightly decreases with temperature due to the thermal activation of the superdislocation motion.

The distribution of the internal critical stresses in the cycled polycrystal was approximated by the Weibull distribution function. These distribution functions are not too different for room temperature straining and high-temperature straining. This shows that the distribution of precipitates in the matrix is not changed substantially. At both temperatures cyclic strain localization which is manifested by the presence of the PSBs in the structure and PSMs on the surface is an important feature. This means that relative small number of volumes participates in a localized cyclic plastic straining.

Localization of cyclic plastic straining has also a decisive effect on the early damage evolution. Thin bands of dislocations cutting both the matrix and γ' precipitates produce parallel PSMs at the surface of individual grains. The character of PSMs has been found very similar to those in simple metals cycled at room temperature. Central extrusion is sometimes accompanied by parallel intrusion, from which fatigue crack starts to grow. In superalloys, the thickness of the extrusion is usually smaller than in simple metals.

For room temperature cyclic straining of nickel superalloys, a characteristic relief of PSMs was observed consisting of central wide ribbon-like extrusion and two thin parallel intrusions (Fig. 5). The thickness of the PSM is approximately the same as that of the PSB found using TEM (see Fig. 6). The dislocation structure of the PSB corresponds to the assumptions of the models of fatigue crack initiation based on the interaction of dislocations in the PSB, formation of point defects and their migration to the matrix [16]. A ladder-like dislocation structure allows a high production of vacancy-type point defects due to localization of the cyclic plastic strain. Supersaturated vacancies created in the walls are annihilated there, but those created in the channels migrate to the neighboring matrix, where they are annihilated at edge dislocations. This results in the transfer of matter between PSB and the matrix. As a result, extrusions and accompanying intrusions arise.

The exact surface relief of PSMs produced by cycling at high temperature could not be assessed due to the oxidation of the surface relief prior to cycling and during cycling. Extrusions produced during cycling oxidize preferably, and thick oxide amplifies the surface relief. Fatigue cracks can initiate in PSMs both for room and high-temperature cycling. However, other damaging mechanisms are present in high temperature cyclic straining. Fatigue cracks can initiate due to oxidation of carbides or by cyclic slip enhancement in or close to grain boundaries and interdendritic areas. The early growth of initiated cracks usually follows. Casting defects affect fatigue crack initiation. The growth of cracks follows PSBs or at high temperature also grain boundaries.

Conclusions. The study of the cyclic stress–strain response, surface relief and internal structure of nickel superalloys cycled at room and at high temperature led to following conclusions:

1. Analysis of the hysteresis loop yields valuable information on the sources of cyclic stress and the distribution of internal critical stresses.

2. Cyclic slip localization in PSBs results in surface relief formation in the form of PSMs at room and high temperatures. Initially, extrusions and (later) accompanying intrusions are formed. The intrusions can transform into to shallow cracks.

3. Dislocation structure of PSBs differs significantly from that of the matrix and witnesses a high dislocation activity in PSBs.

4. Further damaging mechanisms leading to crack initiation, like carbide oxidation and strain localization in grain boundaries or interdendritic areas, are present in high-temperature cyclic straining.

Acknowledgment. The support of the present work by the grants No. 13-23652S and P204/11/1453 of the Grant Agency of the Czech Republic is acknowledged.

Р е з ю м е

Аналіз кривих гістерезису показує, що за різних температур відбуваються характерні зміни залежності між циклічними пластичними деформаціями і напруженнями в нержавіючій сталі і суперсплавах. Відповідні зміни мікрорельєфу поверхні за м'якого навантаження зафіксовано за допомогою сканувальної і томографічної електронної мікроскопії з високим розділенням. Проаналізовано механізми локалізації циклічної деформації, утворення поверхневого мікрорельєфу, ініціювання тріщин від утомленості і росту коротких тріщин.

1. R. Ohtani, "High-temperature fatigue," in: I. Milne, R. O. Ritchie, and B. Karihaloo (Eds.), *Comprehensive Structural Integrity*, Vol. 4, Elsevier, Amsterdam (2003), pp. 327–344.
2. A. Pineau and S. D. Antolovich, "High temperature fatigue of nickel-base superalloys – a review with special emphasis on deformation modes and oxidation," *Eng. Failure Anal.*, **16**, 2668–2697 (2009).
3. M. Petrenec, K. Obrtlík, and J. Polák, "Inhomogeneous dislocation structure in fatigued INCONEL 713LC superalloy at room and elevated temperatures," *Mater. Sci. Eng.*, **A400-401**, 485–488 (2005).
4. J. Polák, "Cyclic deformation, crack initiation, and low cycle fatigue," in: I. Milne, R. O. Ritchie, and B. Karihaloo (Eds.), *Comprehensive Structural Integrity*, Vol. 4, Elsevier, Amsterdam, (2003), pp. 1–39.
5. J. Man, K. Obrtlík, and J. Polák, "Extrusions and intrusions in fatigued metals. Part 1. State of the art and history," *Phil. Mag.*, **89**, 1295–1336 (2009).
6. J. Polák and M. Klesnil, "The hysteresis loop. 1. A statistical theory," *Fatigue Eng. Mater. Struct.*, **5**, 19–32 (1982).
7. G. Masing, "Zur Heyn'schen Theorie der Verfestigung der Metalle durch verborgene elastische Spannungen," *Wiss. Ver. Siemens-Konzern*, **3**, 231–239 (1923).
8. N. N. Afanas'ev, *Statistical Theory of Fatigue Strength of Metals* [in Russian], AN UkrSSR, Kiev (1953).
9. J. Polák, M. Klesnil, and J. Helesic, "The hysteresis loop. 2. An analysis of the loop shape," *Fatigue Eng. Mater. Struct.*, **5**, 33–44 (1982).
10. J. Polák, F. Fardoun, and S. Degallaix, "Analysis of the hysteresis loop in stainless steels. I. Austenitic and ferritic steels," *Mater. Sci. Eng.*, **A297**, 144–153 (2001).

11. J. Polák, F. Fardoun, and S. Degallaix, "Analysis of the hysteresis loop in stainless steels. II. Austenitic-ferritic duplex steel and the effect of nitrogen," *Mater. Sci. Eng.*, **A297**, 154–161 (2001).

12. M. Šmid, M. Petrenec, J. Polák, et al. "Analysis of effective and internal cyclic stress components in the Inconel superalloy fatigued at elevated temperature," *Adv. Mater. Res.*, **278**, 393–398 (2011).

13. R. P. Wahi, J. Auerswald, D. Mukherji, et al. "Damage mechanisms of single and polycrystalline nickel base superalloys SC16 and IN738LC under high temperature LCF loading," *Int. J. Fatigue*, **19**, S89–S94 (1997)

14. K. Obrtlík, A. Chlupova, M. Petrenec, and J. Polák, "Low cycle fatigue of cast superalloy Inconel 738LC at high temperature," *Key Eng. Mater.*, **385-387**, 581–584 (2008).

15. K. Obrtlík, M. Petrenec, J. Man, et al. "Isothermal fatigue behavior of cast superalloy Inconel 792-5A at 23 and 900℃," *J. Mater. Sci.*, **44**, 3305–3314 (2009).

16. J. Polák, "On the role of point defects in fatigue crack initiation," *Mater. Sci. Eng*., **92**, 71–80 (1987).

Received 14. 11. 2013